LWT - Food Science and Technology 42 (2009) 125–130

Contents lists available at ScienceDirect

LWT - Food Science and Technology

journal homepage: www.elsevier.com/locate/lwt

The nanostructure of hemicellulose of crisp and soft Chinese cherry (*Prunus pseudocerasus* L.) cultivars at different stages of ripeness

Fusheng Chen [a], Lifen Zhang [a], Hongjie An [b], Hongshun Yang [a,*], Xiaoyang Sun [a], Hui Liu [a], Yongzhi Yao [a], Lite Li [a]

[a] College of Food Science and Technology, Henan University of Technology, 140 South Songshan Road, Zhengzhou, Henan 450052, PR China
[b] Teda Bio-X center, College of Food Engineering and Biotechnology, Tianjin University of Science & Technology, Tianjin 300457, PR China

ARTICLE INFO

Article history:
Received 7 January 2008
Received in revised form 31 March 2008
Accepted 31 March 2008

Keywords:
Nanostructure
Atomic force microscopy (AFM)
Hemicellulose
Cherry
Ripening

ABSTRACT

Atomic force microscopy (AFM) was used to describe and measure the nanostructure of hemicellulose (HC) samples extracted from two cultivars of Chinese cherry, 'Caode' (soft) and 'Bende' (crisp) at different stages of ripeness. The widths of the HC molecules and aggregates are consistent with little difference between the two cultivars: 23, 29, 34 and 41 nm for ripe soft fruit and 23, 34, 39 and 41 nm for ripe crisp fruit. The results showed that crisp fruit contained a higher percentage of thicker HC chains than soft fruit, suggesting that the thickness of the HC chains may be related to the textural differences observed in the cultivars of the Chinese cherries.

1. Introduction

Texture is considered as the principal quality attribute of fruits that influence acceptability by consumers. The textural changes during ripening are concerned because they directly affect the quality, shelf life, transport capability and disease resistance of fruits. Texture changes of fruits are viewed through alterations in both the cell wall and middle lamella. Structural changes that occur in the middle lamella and primary cell wall during ripening result in cell separation and softening of the tissue. Plant cell walls consist of cellulose microfibrils engaged in a matrix of pectins and hemicelluloses. These polysaccharides form the network of the cell wall and will depolymerize during ripening. The middle lamella is high in pectin and its solubilisation has been correlated with fruit softening during ripening (Barrett & Gonzalez, 1994). In general, pectin and hemicelluloses are the major compositions for textural changes (Yashoda, Prabha, & Tharanathan, 2005). Hemicellulosic polysaccharide plays an important role in the softening process during fruit ripening. The softening process is due to the solubilisation and depolymerisation of pectin and hemicellulose, the relationship between hemicellulose and texture during fruit ripening has been reported by chemical analysis of blueberry (Vicente et al., 2007) and mango (Yashoda et al., 2005). However, cherry has many fundamental different properties from the above mentioned fruits and there are few reports about the effects of hemicellulose on textural changes of cherries (Drake, Kupfermann, & Fellman, 1988; Serrano, Guillen, Martinez-Romero, Castillo, & Valero, 2005), that is hemicellulose is only one of the components which changes during ripening, but that hemicellulose is the molecule of interest in this work. Furthermore, most of the chemical analyses give sample-wide average results and obscure the delicate information (Yang, Wang, Lai, et al., 2007). Investigating the individual structure of molecules is useful and preserving microstructure is important for investigating the spatial arrangement of molecules.

Atomic force microscopy (AFM), as one of the nanotechnology tools, which allows visualization of molecules in the nanorange of magnification, can provide both the qualitative and quantitative structural information for food macromolecules including pectins (Round, Rigby, MacDougall, Ring, & Morris, 2001; Yang, An, Feng, Li, & Lai, 2005; Yang, Feng, An, & Li, 2006; Yang, Lai, An, & Li, 2006) and gelatins (Yang, Wang, Regenstein, & Rouse, 2007). The morphology and surface structures of fruits (Yang, An, Feng, & Li, 2005) and food macromolecular manipulation (Yang, An, & Li, 2006) can also be explored for obtaining more structural information.

Chinese cherry (*Prunus pseudocerasus* L.) is a high-value fruit and good texture is important for obtaining its high marketing value. Cherry can be divided into soft and crisp cultivars, which is similar to most fruits (Batisse, Buret, & Coulomb, 1996). Therefore, cherry was chosen as the material in this research. The objectives of

* Corresponding author. Tel.: +86 371 67789991; fax: +86 371 67756856.
E-mail address: yhsfood@haut.edu.cn (H. Yang).

0023-6438/$34.00
doi:10.1016/j.lwt.2008.03.016

this study were to use AFM to characterize and compare the nanostructures of hemicellulose (HC) in crisp and soft Chinese cherry cultivars at two stages of ripeness.

2. Materials and methods

2.1. Fruits

Two cultivars (soft cultivar 'Caode' and crisp cultivar 'Bende') Chinese cherries (*Prunus pseudocerasus* L.) with two different ripening stages were used for experiment. The ripening stages (unripe and ripe) were determined by experienced farmers. The ripe cherry was selected according to the requirement of commercial maturity. Cherries are nonclimacteric fruits. Therefore, the ripe fruit was picked at pick maturity, judged mainly from skin color (Gonçalves et al., 2004). And the unripe cherry was picked about one week before ripe. The two cultivars were hand-picked at a farm in Zhengzhou, Henan province, China, and transported to the laboratory in 2 h. Fruits with uniform size, disease free and no other defects were selected. The 'Caode' was named as 'soft cherry' and the 'Bende' was named as 'crisp cherry' in the following text according to their textural difference.

2.2. Cell wall preparation and determination of HC

Cell wall material of cherry flesh was extracted according to the methods described by Deng, Wu, and Li (2005) with modification (Fig. 1). About 10 g cherry flesh (from about 20–30 peeled and pitted fruits for evenly sampling) was rapidly pestled in an ice-cold mortar, then transferred into boiling ethanol (Tianjin Resent Chemicals Co., Ltd, China) for 20 min. After filtration, the residue was extracted again with the ethanol for two times. And all the following extraction steps are repeated three times and collected together. Then the residue was incubated with dimethylsulphoxide (DMSO, Tianjin Resent Chemicals Co., Ltd, China):water (volume ratio was 9:1) for removing starch. Then it was washed by water and transferred to chloroform (Suzhou Chemicals Co., Ltd, China):ethanol (2:1). The sample was filtrated and washed with 200 mL acetone (Luoyang Chemicals Co., Ltd, China) until whitening totally, and then the cell wall material was obtained. For extracting HC, the cell wall material was dissolved in sodium acetate (Luoyang Chemicals Co., Ltd, China) buffer. After centrifugation, the water-insoluble pellet was transferred to sodium acetate buffer with *trans*-1,2-diaminocyclohexane-*N*,*N*,*N*′,*N*′-tetraacetic acid (CDTA) (Tianjin Zinco Fine Chemical Institute, China). The residue was re-suspended in Na_2CO_3/CDTA, shaken and centrifuged as above. The final extraction was carried out using NaOH/$NaBH_4$ (Sinopharm Chemical Reagent Co., Ltd, China). The solution was centrifuged as above and the extraction was repeated twice. The filtrates from the three consecutive extractions were pooled and referred to as hemicellulose fraction (HC). To compare our results with the literature another sample of cell wall material from ripe crisp fruit was extracted using potassium oxalate (Tianjin Kermel Chemical Reagent Co., Ltd, China) instead of sodium acetate/CDTA, while the other steps were the same as above (Thomas & Thibault, 2002). This sample was defined as ripe crisp fruit 2.

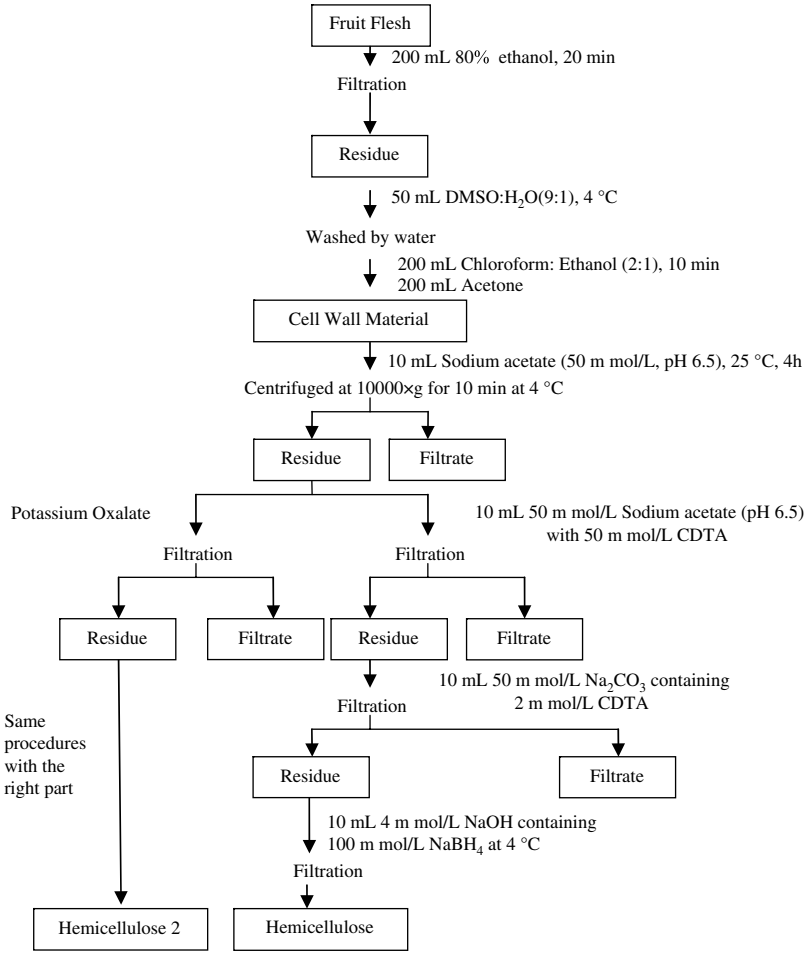

Fig. 1. Scheme for extraction of hemicellulose fractions from Chinese cherry.

The HC content of Chinese cherry was determined by the anthrone colorimetry method (Deng et al., 2005; Han, 1992). Glucose (Sigma Co., Ltd, USA) was used as standard. HC solution (2 mL) was mixed with 0.5 mL of anthrone reagent (Tianjin Kermel Chemical Reagent Co., Ltd, China) in a test-tube, then 5 mL sulfuric acid (Luoyang Chemicals Co., Ltd, China) was added to the mixture system. Then, the mixture was boiled for 5 min and cooled with running tap water immediately. The mixed solution was incubated at room temperature for 10 min, then the absorbance at 620 nm (A_{620nm}) was measured with a UV-2000 spectrophotometer (Unico (Shanghai) Instrument Co., Ltd) at room temperature.

2.3. AFM determination and image analysis

The nanostructural characterization of HC was performed in air using an AFM (JSPM-5200, JEOL, Japan) in AC mode. The method was from previous research with slight modification (Yang, An, Feng, Li, & Lai, 2005; Yang, Feng, et al., 2006; Yang, Lai, et al., 2006). HC fractions were diluted to a series of concentrations for obtaining a reasonable concentration for imaging (about 0.5–30 μg/mL). The diluted solutions were agitated with a Vortex mixer (Fisher Scientific, Pittsburgh, PA, USA). A small volume (10–20 μL) of the solutions was pipetted onto freshly cleaved mica surface, and dried in air. The NSC 11/no Al (MikroMasch, Wilsonville, OR, USA) tip was used. The resonance frequency of the tip is about 330 kHz and the force constant is 48 N/m. (Yang, Wang, Regenstein, et al., 2007).

AFM offline software (WinSPM System, Japan) was applied to analyze the AFM images. The images were corrected with flattening to improve the visual quality. The bright and dark areas in the images corresponded to peaks and troughs of the imaged chains, respectively, as shown in height scale (15 nm). Height mode images were analyzed, which included both 2-dimentional (plane) and 3-dimentional (3D) images. The quantitative information of the uncorrected images including the width and height of the HC molecules and aggregates was determined by section analysis (Yang, Wang, Regenstein, et al., 2007).

2.4. Statistical analysis

Two independent extractions of cell wall materials were conducted for each group and HC determinations were conducted in triplicate for each extraction. Because of little variation in the triplicate results in each extraction, the average results of the two extractions were used for statistical analysis. Parallel AFM images (10–15) were analyzed for each specimen for acquiring reliable and statistically valid results. The qualitative data of HC contents and chain heights were recorded as means ± standard deviations. Analysis of variance (ANOVA) ($P < 0.05$) and Duncan's multiple range test for differences among different groups were performed using SAS 9.1.3 software (SAS, Cary, NC, USA). Comparisons that yielded P values <0.05 were considered significant.

3. Results and discussion

3.1. Effects of ripening stages and cultivars on HC contents of Chinese cherry

Table 1 shows that the HC content decreased with the ripening of cherry fruit. During fruit ripening, for 100 g flesh weight, the HC content decreased from 10.8 to 4.5 mg for the soft fruit, and from 11.8 to 5.4 mg for the crisp fruit, and this was consistent with other reports (Jain, Dhawan, Malhotra, & Singh, 2003; Rosli, Civello, & Martínez, 2004). The decrease in HC content was attributed to the increase in the activities of cell wall hydrolyzing enzymes (Jain et al., 2003). The HC contents of the crisp fruits at two ripening stages were slightly higher than those of the corresponding soft fruit. There was no statistical difference between the HC contents of the two samples that were obtained from the two methods (Table 1). The decrease of HC was consistent with the softening process of fruit, which could be viewed as solubilisation and depolymerisation.

Table 1
Effects of cultivars and ripening stages on the hemicellulose contents of Chinese cherry

Samples	Unripe soft fruit	Ripe soft fruit	Unripe crisp fruit	Ripe crisp fruit	Ripe crisp fruit 2
Hemicellulose (mg)	10.8 ± 0.5^a	4.5 ± 0.6^b	11.8 ± 1.8^a	5.4 ± 0.1^b	4.8 ± 0.7^b

Note. Different letters (a, b) in the same row indicate significant ($P < 0.05$) differences among different extraction temperatures. The flesh weight was 100 g for each group.

3.2. HC nanostructures of the two Chinese cherry cultivars at two ripening stages

Figs. 2–4 show the AFM images of Chinese cherry HC in different groups. All the structures of HC molecules were similar to "broom". The AFM images showed that there were many branches on one main chain, or new branches formed on existing branches (Figs. 2d and e and Figs. 3d and e). This might be attributed to the tangled network of polysaccharide molecules (Yan & Zhu, 2003). The differences among the nanostructure of HC from the two cultivars during fruit ripening could also be seen by comparing the images. The HC molecule branches of the ripe crisp fruit all oriented in the same direction (Fig. 3). However, the orientation of HC molecule branches of the ripe soft fruit was irregular (Fig. 2a and b). The AFM shows not only the plane images of HC molecules but also the three-dimensional images which can better present the results. For example, Figs. 2f, 3f and 4d were corresponding 3D images of Figs. 2e, 3e and 4c, respectively. The details of the images could be viewed more clearly through enlargement. For example, Fig. 2e was the enlargement of the rectangle part of Fig. 2d. For unripe groups, the HC might aggregate into large aggregates with other materials and could not be successfully imaged by AFM. For the HC extracted from different methods, CDTA extracted HC remained associated together, while oxalate extracted HC was more dissociated, which was consistent with the report by Thomas and Thibault (2002).

The quantitative characteristics of HC molecules in different groups were obtained by AFM software. The color bar legends on the right of images were used for showing the height values in z-scale. In Figs. 2–4, all z-range of these images was 15 nm for easy comparison. Fig. 5 shows the section analysis of the HC molecules and aggregates. As shown in Fig. 5, the width (W) and the corresponding height (V) of the HC chains were determined by the software. Here, V was recorded by the height of HC chains relative to the mica plane surface, W was calculated by the width of chain half height for improving data precision, and was about the half of the value of the definition for peach pectin analysis (Yang, An, Feng, Li, & Lai, 2005, Yang, Feng, et al., 2006; Yang, Lai, et al., 2006). Fq was recorded as number of times that special chain widths occurred. The Fq and V values of different widths of chains (W) in ripe fruit were shown in Table 2. From Table 2, the widths of chains from section analysis reflected that the chain widths (W) had dozens of discrete values. However, these values were composed of several basic ones: 23, 29, 34 and 41 nm for the ripe soft fruit, and 23, 34, 39 and 41 nm for the ripe crisp fruit. The widths of other chains in both cultivars were all composed of these values, respectively. For example, 47, 68, 78 and 83 nm were approximately twice that of 23, 34, 39 and 41 nm, respectively. Number of 54 nm was approximately the sum of 23 and 29 nm. It should be noted that once there were too many branch chains of the HC molecules associating

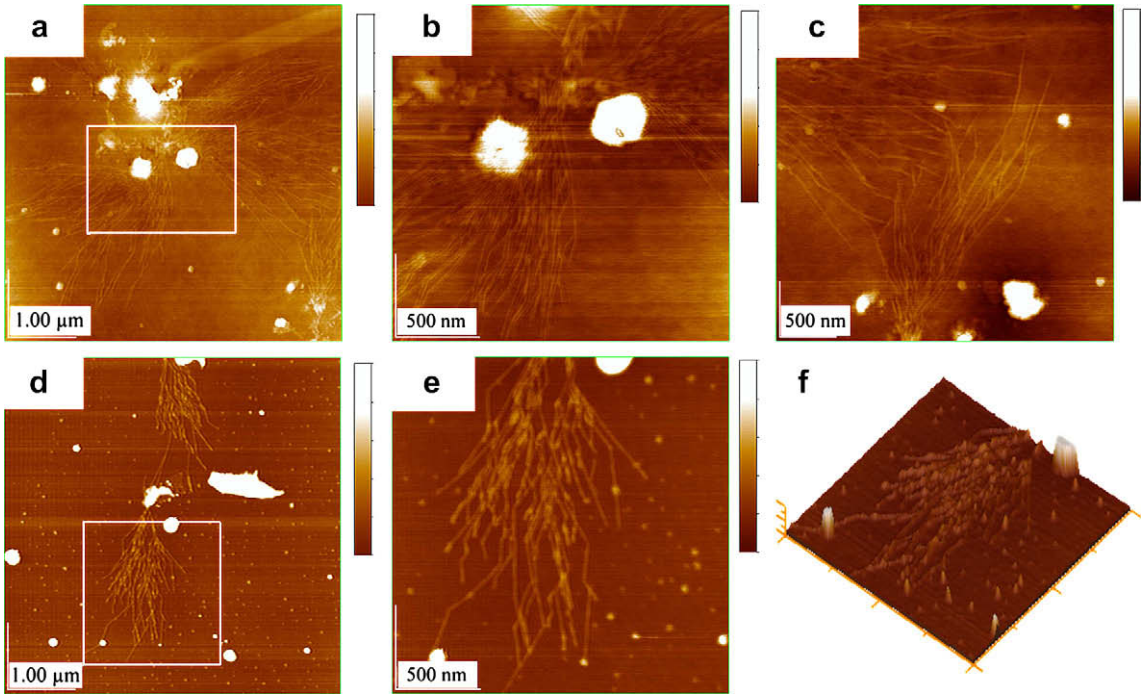

Fig. 2. AFM images of hemicellulose from soft ripe Chinese cherry. Height bar = 15 nm. (a) atypical image, area: 5.00 × 5.00 μm^2; (b) zoom plane image in the marked region of (a), area: 2.00 × 2.00 μm^2; (c) localized image, area: 3.00 × 3.00 μm^2; (d) typical image, area: 5.00 × 5.00 μm^2; (e) and (f) zoom plane and 3D images in the marked region of (d), area: 2.00 × 2.00 μm^2.

together, some molecules aggregated into spherical aggregates and did not separate well into distinct small aggregates. These chains could not be separated from images, determined by the software precisely and the lengths of these chains would be excluded for statistical analysis. The lengths of main chains were about 2–5 μm, and the lengths of branch chains were about 100 nm to 2 μm. The lengths were longer than those from straw (Yan & Zhu, 2003).

Compared the soft fruit to crisp one, there was significant difference between the chain widths (Table 2), the relative percentages of large widths of crisp fruit were larger than that of soft group. However, for *V* values, crisp group 1 was significant larger than those of other two groups. Therefore, it was the chain widths (*W*) rather than the chain heights (*V*) that had a closer relationship with the texture properties of Chinese cherry.

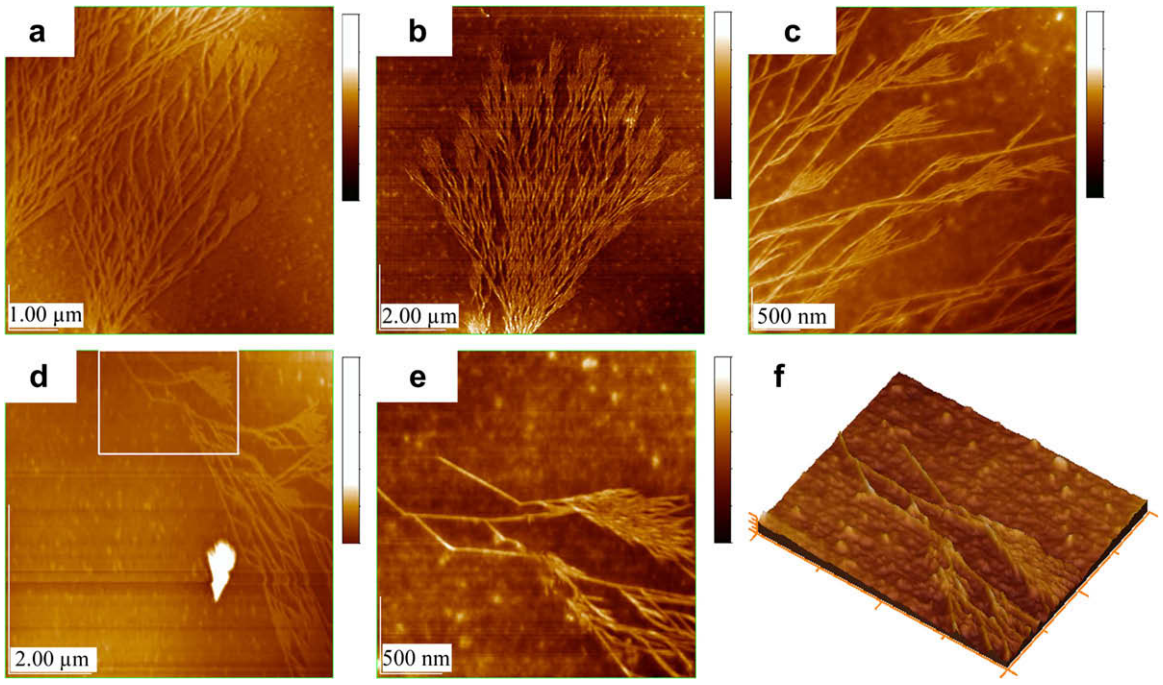

Fig. 3. AFM images of hemicellulose from crisp ripe Chinese cherry. Height bar = 15 nm. (a) atypical image, area: 6.66 × 7.16 μm^2; (b) typical image, area: 10.00 × 10.00 μm^2; (c) localized image, area: 3.44 × 3.80 μm^2; (d) localized image, area: 7.98 × 3.97 μm^2; (e) and (f) zoom plane and 3D images in the marked region of (d), area: 2.60 × 2.11 μm^2.

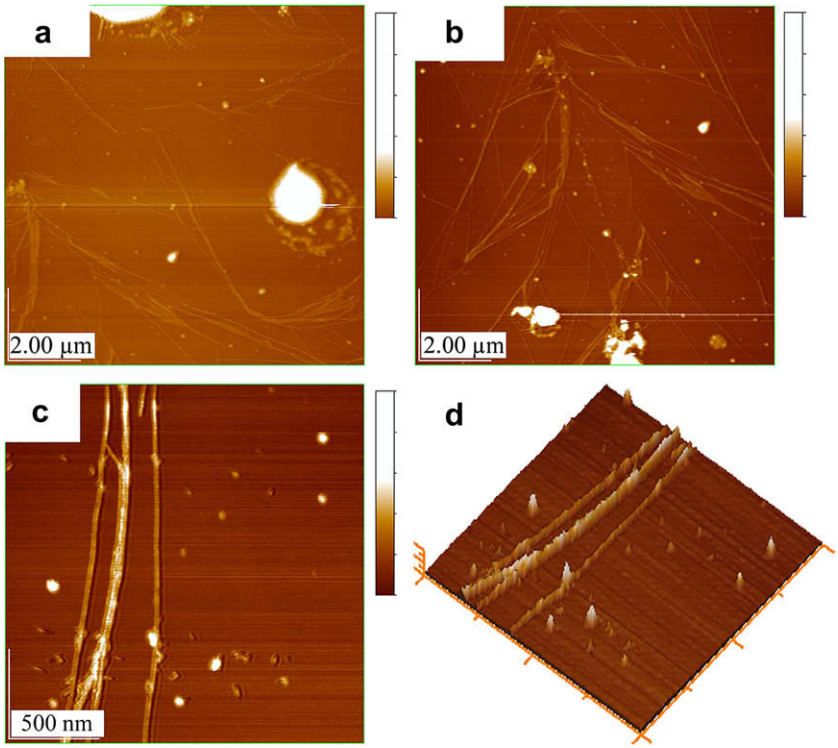

Fig. 4. AFM images of hemicellulose 2 from crisp ripe Chinese cherry. Height bar = 15 nm. (a) atypical image, area: 10.00 × 10.00 μm^2; (b) typical image, area: 10.00 × 10.00 μm^2; (c) localized image, area: 2.00 × 2.00 μm^2; (d) 3D image of (c), area: 2.00 × 2.00 μm^2. Note: the sample was ripe crisp fruit 2 (or called hemicellulose 2 in Fig. 1).

3.3. *Relationship between the HC nanostructures and cultivars and ripening stages of Chinese cherry*

Texture directly influences the shelf life of fruits and maintaining a reasonable firmness is very important for fruit quality control. The texture properties are closely related to the cultivars and ripening stages. Previous research indicated that textural changes are closely related to the structures and contents of hemicellulose (Barrett & Gonzalez, 1994; Yashoda et al., 2005; Vicente et al., 2007).

The texture change in fruits is a consequence of modifications undergone by component polysaccharides, which give rise to disassembly of primary cell wall and middle lamella structures. Hemicellulose is responsible for the alteration of cell wall structure during fruit ripening (Barrett & Gonzalez, 1994; Jain et al., 2003; Manrique & Lajolo, 2004). However, the role of hemicelluloses in the softening process during fruit ripening has not yet been elucidated (Manrique & Lajolo, 2004). There were no significant differences for the contents of HC and *V* values of the nanostructural HC chains in different cultivars (soft and crisp), but the values of HC widths were significantly larger in crisp groups than those in soft groups (Table 2), which revealed that the widths of the nanostructural HC might account for the textural difference between cultivars of Chinese cherry.

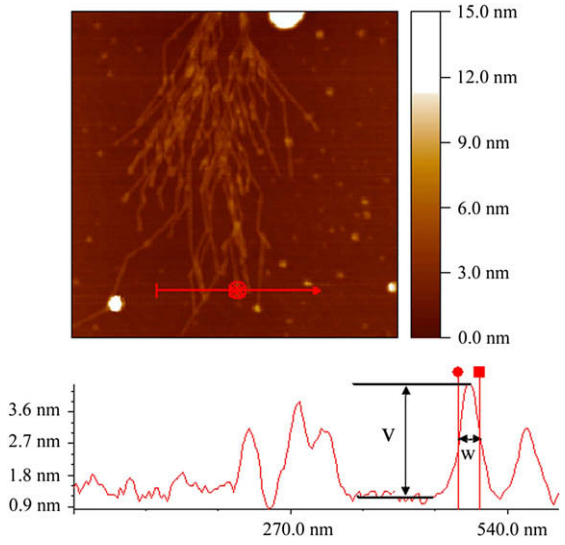

Fig. 5. Section analysis of hemicellulose chains. Note: *W*: chain width calculated by the peak width of chain half height; *V*: height of hemicellulose chain.

Table 2
Frequency and vertical distances of chain widths of Chinese cherry hemicelluloses

W (nm)	Ripe soft fruit		Ripe crisp fruit		Ripe crisp fruit 2	
	Fq	*V* (nm)	Fq	*V* (nm)	Fq	*V* (nm)
23	12	1.06 ± 0.51	–	–	–	–
29	18	1.71 ± 0.97	–	–	–	–
34	10	1.19 ± 0.64	3	3.85 ± 1.76	–	–
39	–	–	3	3.74 ± 2.00	3	1.39 ± 0.66
41	7	1.81 ± 1.59	7	4.61 ± 1.50	–	–
47	8	1.09 ± 0.31	10	3.09 ± 1.98	1	0.789 ± 0
54	–	–	4	5.22 ± 1.83	2	2.04 ± 1.03
62	–	–	4	1.79 ± 0.78	3	1.70 ± 1.01
68	4	1.17 ± 0.09	4	1.80 ± 2.29	–	–
78	–	–	10	1.65 ± 0.99	7	0.94 ± 0.63
83	–	–	8	1.89 ± 1.03	6	1.03 ± 1.57
94	–	–	13	1.95 ± 1.03	11	0.85 ± 0.38
109	–	–	7	2.10 ± 0.87	8	0.79 ± 0.30
124	–	–	3	3.05 ± 0.31	4	1.37 ± 0.47
136	–	–	2	3.37 ± 0.74	–	–
146	–	–	1	3.06 ± 0	4	1.13 ± 0.68
153	–	–	1	4.26 ± 0	–	–
172	–	–	–	–	2	1.95 ± 0.40

Note. *W*: the peak width of half height of HC chains; *V*: the height of hemicellulose chains; Fq: refers to the numbers of times particular chain widths were observed.

4. Conclusions

Content and nanostructures of HC from two cultivars Chinese cherry at unripe and ripe stages were determined to illustrate the fundamental of the quality difference among cherry fruits. The widths of the cherry HCs were very regular, almost all of the widths of HC molecules of ripe fruits were composed of four basic values: 23, 29, 34 and 41 nm for the soft fruit and 23, 34, 39 and 41 nm for the crisp fruit. The results showed that crisp fruit contained a higher percentage of thicker HC chains than soft fruit, indicating that the thickness of the HC chains may be related to the textural differences observed in the cultivars of the Chinese cherries.

Acknowledgements

Project 30600420 supported by National Natural Science Foundation of China contributed to this research. We also acknowledge the financial support (No. 0200082) from Tianjin University of Science and Technology.

References

Barrett, D. M., & Gonzalez, C. (1994). Activity of softening enzymes during cherry maturation. *Journal of Food Science, 59*, 574–577.

Batisse, C., Buret, M., & Coulomb, P. J. (1996). Biochemical differences in cell wall of cherry fruit between soft and crisp fruit. *Journal of Agricultural and Food Chemistry, 44*, 453–457.

Deng, Y., Wu, Y., & Li, Y. (2005). Changes in firmness, cell wall composition and cell wall hydrolases of grapes stored in high oxygen atmospheres. *Food Research International, 38*, 769–776.

Drake, S. R., Kupferman, E. M., & Fellman, J. K. (1988). 'Bing' sweet cherry (*Prunus avium* L.) quality as influenced by wax coatings and storage temperature. *Journal of Food Science, 53*, 124–126, 156.

Gonçalves, B., Landbo, A. K., Knudsen, D., Silva, A. P., Moutinho-Pereira, J., Rosa, E., et al. (2004). Effect of ripeness and postharvest storage on the phenolic profiles of cherries (*Prunus avium* L.). *Journal of Agricultural and Food Chemistry, 52*, 523–530.

Han, Y. S. (1992). *Experimental guidance of food chemistry*. Beijing: Beijing Agriculture University Press. pp. 5–8.

Jain, N., Dhawan, K., Malhotra, S., & Singh, R. (2003). Biochemistry of fruit ripening of guava (*Psidium guajava* L): compositional and enzymatic changes. *Plant Foods for Human Nutrition, 58*, 309–315.

Manrique, G. D., & Lajolo, F. M. (2004). Cell-wall polysaccharide modifications during postharvest ripening of papaya fruit (*Carica papaya*). *Postharvest Biology and Technology, 33*, 11–26.

Rosli, H. G., Civello, P. M., & Martínez, G. A. (2004). Changes in cell wall composition of three Fragaria × ananassa cultivars with different softening rate during ripening. *Plant Physiology and Biochemistry, 42*, 823–831.

Round, A. N., Rigby, N. M., MacDougall, A. J., Ring, S. G., & Morris, V. J. (2001). Investigating the nature of branching in pectin by atomic force microscopy and carbohydrate analysis. *Carbohydrate Research, 331*, 337–342.

Serrano, M., Guillen, F., Martinez-Romero, D., Castillo, S., & Valero, D. (2005). Chemical constituents and antioxidant activity of sweet cherry at different ripening stages. *Journal of Agricultural and Food Chemistry, 53*, 2741–2745.

Thomas, M., & Thibault, J. F. (2002). Cell-wall polysaccharides in the fruits of Japanese quince (*Chaenomeles japonica*): extraction and preliminary characterisation. *Carbohydrate Polymers, 49*, 345–355.

Vicente, A. R., Ortugno, C., Rosli, H., Powell, A. L. T., Greve, L. C., & Labavitch, J. M. (2007). Temporal sequence of cell wall disassembly events in developing fruits. 2. Analysis of blueberry (*Vaccinium* species). *Journal of Agricultural and Food Chemistry, 55*, 4125–4130.

Yan, L., & Zhu, Q. (2003). Direct observation of the main cell wall components of straw by atomic force microscopy. *Journal of Applied Polymer Science, 88*, 2055–2059.

Yang, H., An, H., Feng, G., & Li, Y. (2005). Visualization and quantitative roughness analysis of peach skin by atomic force microscopy under storage. *LWT-Food Science and Technology, 38*, 571–577.

Yang, H., An, H., Feng, G., Li, Y., & Lai, S. (2005). Atomic force microscopy of the water-soluble pectin of peaches during storage. *European Food Research Technology, 220*, 587–591.

Yang, H., An, H., & Li, Y. (2006). Manipulate and stretch single pectin molecules with modified molecular combing and fluid fixation techniques. *European Food Research Technology, 223*, 78–82.

Yang, H., Feng, G., An, H., & Li, Y. (2006). Microstructure changes of sodium carbonate-soluble pectin of peach by AFM during controlled atmosphere storage. *Food Chemistry, 94*, 179–192.

Yang, H., Lai, S., An, H., & Li, Y. (2006). Atomic force microscopy study of the ultrastructural changes of chelate-soluble pectin in peaches under controlled atmosphere storage. *Postharvest Biology and Technology, 39*, 75–83.

Yang, H., Wang, Y., Lai, S., An, H., Li, Y., & Chen, F. (2007). Application of atomic force microscopy as a nanotechnology tool in food science. *Journal of Food Science, 72*, R65–R75.

Yang, H., Wang, Y., Regenstein, J. M., & Rouse, D. B. (2007). Nanostructural characterization of catfish skin gelatin using atomic force microscopy. *Journal of Food Science, 72*, 430–440.

Yashoda, H. M., Prabha, T. N., & Tharanathan, R. N. (2005). Mango ripening – chemical and structural characterization of pectic and hemicellulosic polysaccharides. *Carbohydrate Research, 340*, 1335–1342.